ChemPubSoc Europe

DOI: 10.1002/cssc.201902341

CHEMSUSCHEM Communications

Melamine-Based Microporous Organic Framework Thin Films on an Alumina Membrane for High-Flux Organic Solvent Nanofiltration

Mohammad Amirilargani,*[a] Giovana N. Yokota,[a] Gijs H. Vermeij,[a] Renaud B. Merlet,[d] Guusje Delen,[c] Laurens D. B. Mandemaker,[c] Bert M. Weckhuysen,[c] Louis Winnubst,[d] Arian Nijmeijer,[d] Louis C. P. M. de Smet,*[a, b] and Ernst J. R. Sudhölter*[a]

Microporous polymer frameworks have attracted considerable attention to make novel separation layers owing to their highly porous structure, high permeability, and excellent molecular separation. This study concerns the fabrication and properties of thin melamine-based microporous polymer networks with a layer thickness of around 400 nm, supported on an α-alumina support and their potential use in organic solvent nanofiltration. The modified membranes show excellent solvent purification performances, such as *n*-heptane permeability as high as 9.2 $L\,m^{-2}\,h^{-1}\,bar^{-1}$ in combination with a very high rejection of approximately 99% for organic dyes with molecular weight of $\geq$457 Da. These values are higher than for the majority of the state-of-the-art membranes. The membranes further exhibit outstanding long-term operation stability. This work significantly expands the possibilities of using ceramic membranes in organic solvent nanofiltration.

Purification of organic solvents has received much attention, owing to increasing environmental concerns and the search for cleaner and more energy-efficient processes.[1] Organic solvent nanofiltration (OSN) is an energy-efficient, membrane-based separation process with a high potential to be employed in a wide range of applications.[2] However, the development of high-performance OSN processes remains challenging. Despite the satisfactory rejection by OSN membranes reported to date, most of them have relatively low solvent permeabilities. Reduction of the selective layer thickness is an obvious means of enhancing the solvent permeability. Such a path length reduction has been applied to graphene-based membranes,[1c,3] bilayer polyelectrolyte membranes,[4] and interfacially polymerized polyamide membranes,[5] all resulting in a significant increase in solvent permeation.

Membranes with molecular sieving properties, originating from the presence of well-ordered and tunable pores are attractive candidates for OSN where high molecular size selectivity for rejection in combination with high solvent permeation is required.[6] Microporous materials, such as metal–organic frameworks (MOFs),[6b,7] zeolites,[8] and graphene,[1c,9] are well-known molecular sieve materials, showing high permeability and selectivity. Recently, a wide range of porous all-organic frameworks have become of interest for investigations in membrane applications. Among these are the porous organic frameworks (POFs),[10] crystalline covalent organic frameworks (COFs),[6a,11] covalent triazine frameworks (CTFs),[12] polymers of intrinsic microporosity (PIMs),[13] porous aromatic frameworks (PAFs),[14] and amorphous hyper-crosslinked polymers (AHCPs).[15] The use of POFs has recently received tremendous attention in the field of molecular sieving membranes.[16] Polycondensation of melamine and aromatic *bis*-aldehydes results in the formation of a microporous polymer network of aminal bonds.[17] Schiff-base-based POFs were found to be chemically stable in polar and nonpolar organic solvents, in aqueous solution with a wide range of pH (2.0–13.0), and even under extreme harsh conditions, like boiling water.[18] Interestingly, recently developed POFs made from melamine and terephthaldehyde, having a mean pore diameter of approximately 5 Å, have shown very good properties for nanofiltration[19] and gas separation applications.[15]

Herein we report the direct formation of a thin POF layer supported by an α-alumina ceramic membrane. The α-alumina, with an average pore diameter of 80 nm, was first modified with 3-aminopropyl trimethoxy silane (APTES), to promote covalent linkage of the in situ-prepared POF in the subsequent step (Figure 1). In more detail, this step involves a polycondensation on top of the amine-functionalized α-alumina membrane using melamine and terephthaldehyde (i.e., benzene

[a] M. Amirilargani, G. N. Yokota, G. H. Vermeij, Dr. L. C. P. M. de Smet, Prof. Dr. E. J. R. Sudhölter
Department of Chemical Engineering, Delft University of Technology
Van der Maasweg 9, 2629 HZ Delft (The Netherlands)
E-mail: m.amirilargani@tudelft.nl
louis.desmet@wur.nl
e.j.r.sudholter@tudelft.nl

[b] Dr. L. C. P. M. de Smet
Laboratory of Organic Chemistry, Wageningen University & Research
Stippeneg 4, 6708 WE Wageningen (The Netherlands)
E-mail: louis.desmet@wur.nl

[c] G. Delen, L. D. B. Mandemaker, Prof. Dr. B. M. Weckhuysen
Debye Institute for Nanomaterials Science, Utrecht University
Universiteitweg 99, 3584 CG Utrecht (The Netherlands)

[d] R. B. Merlet, Prof. Dr. L. Winnubst, Prof. Dr. A. Nijmeijer
Inorganic Membranes, MESA+ Institute for Nanotechnology
University of Twente, P.O. Box 217, 7500 AE Enschede (The Netherlands)

Supporting Information and the ORCID identification number(s) for the author(s) of this article can be found under: https://doi.org/10.1002/cssc.201902341.

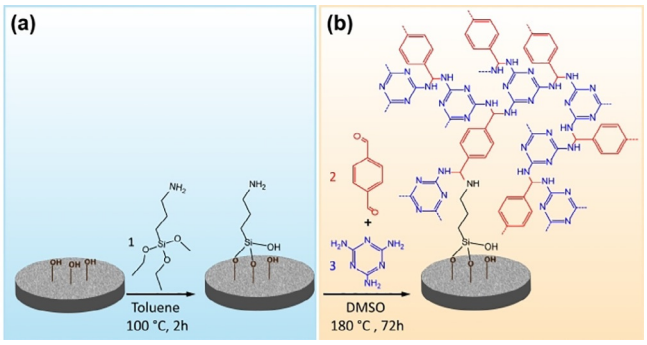

Figure 1. a) Grafting of APTES onto the α-alumina membrane. b) In situ synthesis of melamine–terephthaldehyde microporous polymer networks (MT POF) on the APTES-modified α-alumina membrane. Molecules **1**, **2**, and **3** are APTES, terephthaldehyde and melamine, respectively.

1,4-dicarboxaldehyde) to make a melamine–terephthaldehyde (MT) POF thin film. To study the effect of the *bis*-aldehyde's structure on the morphology and performance of the thin membrane, we also used *iso*-phthaldehyde (i.e. benzene 1,3-dicarboxaldehyde) as a POF building block to synthesize a melamine–*iso*-phthaldehyde (MI) POF thin film. The polycondensation reaction resulted in a light yellow coloration of the α-alumina membrane, which remained after thoroughly washing with THF and acetone (Figure 2a).

Next, the POF-modified membranes were investigated by both surface and cross-sectional field-emission scanning electron microscopy (FESEM) and compared to the images obtained from the unmodified, bare membranes. For the unmodified α-alumina membrane, the FESEM image of the surface (Figure 2b) shows the typical surface morphology, reflecting closely packed micro-sized α-alumina particles, while it can be clearly seen that the membrane surface morphology changed upon the POF-formation. The cross-sectional images (Figure 2c,d) show a thin "blanket" of the MT POF, with a thickness of around 400 nm. For the membranes modified with MI POFs, the cross-sectional FESEM image displays a similar morphology and a thickness of around 450 nm.

To learn more about the (network) structure of the synthesized POF layer, the MT POF-modified α-alumina membranes were also characterized by an emerging tip-sensed AFM-IR technology, namely, photo-induced force microscopy (PiFM). In PiFM-IR, a pulsed laser source induces a dipole in the POF layer and consequently a mirror dipole is induced in the AFM tip, which is translated into FT-IR spectral data.[20] Details on the experimental approaches used can be found in the Supporting Information.

The 3D surface morphology of the MT POF-modified α-alumina membrane shows a rather dense structure of the membrane surface, whereas the POF particles are clearly visible at the surface (Figure 2f). We randomly chose five points at the surface for FT-IR analysis (Figure 2g). The obtained FT-IR spectra all manifest two strong bands at 1480 and 1542 cm^{-1}, which are attributed to the semicircle and quadrant stretching of the triazine ring in the POF structure, respectively. These peaks are similar to those from the FT-IR analysis of the MT

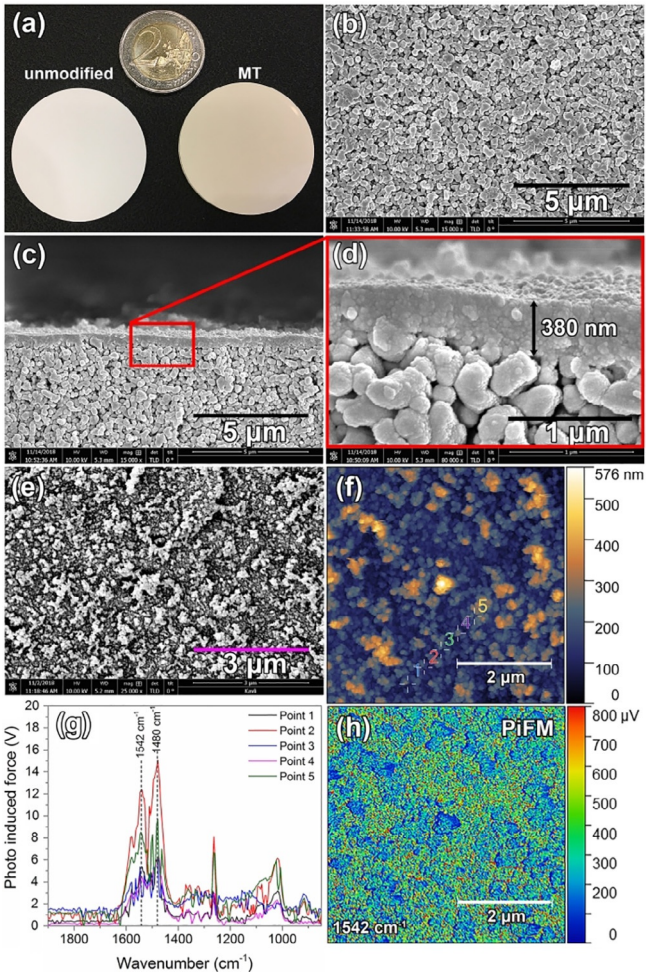

Figure 2. a) Photographs of unmodified and MT POF-modified α-alumina membranes. b) Surface FESEM image of unmodified membrane. c) Low-magnification cross-section FESEM image, d) high-magnification cross-section FESEM image, e) surface FESEM, f) 3D AFM surface image, g) Surface FT-IR analysis, and h) FT-IR image of MT POF-modified α-alumina membrane.

POF powders (see the Supporting Information, Figure S4), indicating a certain level of similarity in the chemical structure of the POF films and the collected POF powders. As can be seen in the FT-IR map taken at 1542 cm^{-1}, as well as the point analysis (Figure 2h), the POF thin film is homogeneously dispersed at the surface of the α-alumina support.

Once the presence of the thin MT-POF films was confirmed, their solvent stability is among the most important factors having a crucial impact as it can cause severe swelling or even dissolution of the membrane materials, resulting in loss of separation performance. Therefore, we examined the stability of the POF powders when dispersed in toluene and *n*-heptane for a period of up to four weeks. Since no changes from the FT-IR spectra were observed in this time (Figure S4), we conclude that these POFs are stable in contact with these solvents.

From N_2 adsorption–desorption experiments on the POF powders, the BET surface was determined to be 520 $m^2 g^{-1}$ for the MT POF and 598 $m^2 g^{-1}$ for MI POF. By using a nonlocal density functional theory (NL-DFT) method, pore diameters of

approximately 5 and 4 Å were calculated for the corresponding POFs (Figure S5), indicating their microporous structures.

To date there has been little success in making membranes that show high solvent permeability in combination with high solute rejection for nonpolar organic solvents, such as toluene and *n*-heptane. These solvents have tremendous applications and are therefore ideal choices for OSN performance tests using different molecular weight dyes.[21] We have investigated OSN performance of the MT and MI POF-modified α-alumina membranes using a solution of toluene and *n*-heptane containing 20 mg L^{-1} Sudan Red 7B (M_W = 379 Da), Solvent Green 3 (M_W = 418 Da), Sudan Black B (M_W = 456 Da) and Bromothymol Blue (M_W = 624 Da; Figure S7 and Table S1).

The results of the measured rejection of organic dyes and the solvent permeability are shown in Figure 3. For the MT and MI POF-modified α-alumina membranes with toluene as the solvent, a solute rejection of ≥90% was found for Solvent Green 3, Sudan Black B, and Bromothymol Blue, whereas Sudan Red 7B shows a rejection of around 50%. With *n*-heptane as the solvent, the results were very similar, although the rejections for Solvent Green 3 and Sudan Red 7B were somewhat lower. In both cases, the solvent permeability remains high (i.e., 6–8 L m^{-2} h^{-1} bar^{-1}). For *n*-heptane, the permeability

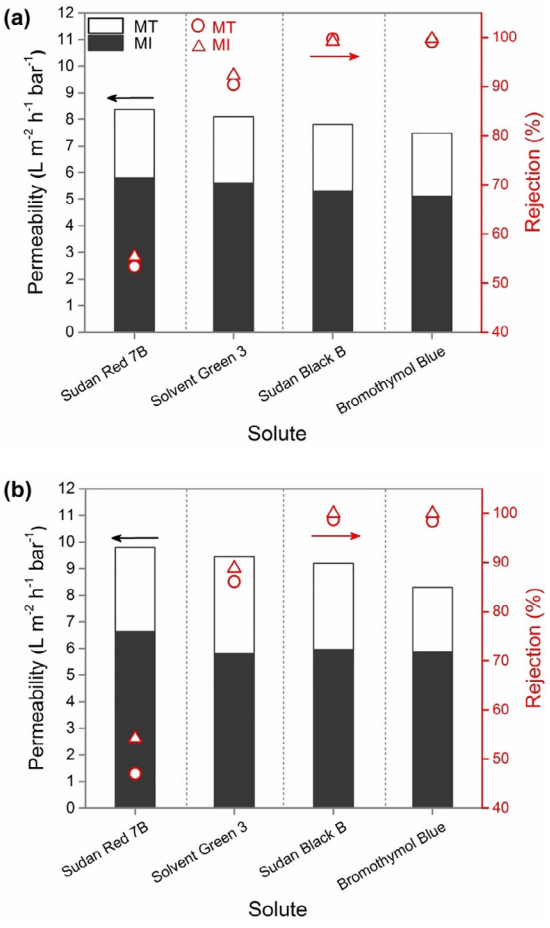

Figure 3. Solvent permeability (columns) and solute rejection (red markers) for MT and MI POF-modified α-alumina membranes in (a) toluene and (b) *n*-heptane.

was always a few percent higher than for toluene (Figure 3), which can be attributed to the difference in the solvent dynamic viscosity (0.37 MPa s and 0.59 MPa s for *n*-heptane and toluene, respectively) and their kinetic diameters (4.3 Å[22] and 5.8 Å,[23] respectively).

From Figure 3 it can also be clearly seen that the solvent permeability found for the MI POF-modified α-alumina membranes is lower than that for the MT POF-modified α-alumina membranes. This is attributed to a roughly 50 nm thicker layer of MI POF compared with that of MT POF and the somewhat denser structure of the MI POF-modified α-alumina membrane (Figure S6). Both POF-modified membranes show very high rejections (≥90%) of solute molecules of a M_W ≥ 418 Da in toluene, whereas the rejections in *n*-heptane of Solvent Green 3, with a M_W of 418 Da, are 86 and 89% for MT and MI POFs-modified α-alumina membranes, respectively. It is important to note that the pore sizes of the POF-modified membranes are expected to be lower than the size of a Solvent Green 3 molecule. Unfortunately, effective solute diameters, which can be calculated in different ways, are not always accessible. For example, to calculate the Stokes diameter, the solute diffusivity in each solvent is needed.[24] Nevertheless, from the solute molecular weight point of view, our results signify that the molecular weight cut-off (MWCO) of our membranes is around 460 Da.

The long-term stability of the MT membrane was characterized by measuring the toluene and *n*-heptane permeability and Bromothymol Blue rejection (Figure 4). Both remained constant during 12 h of measurement, indicating high solvent stability for the POF membranes for this system.

Finally, we compared our new MT POF-modified α-alumina membranes for separation of Sudan Black B from toluene and *n*-heptane with reported functionalized ceramic membranes and the commercially available polymeric STARMEM 122 membranes. For all these systems, the observed rejections were plotted against their respective permeabilities (Figure 5). The rejection and permeability properties of our system are exceptionally high compared to those of the other systems. This is a direct consequence of the thickness of only 380 nm of the POF layer on the α-alumina supporting membrane of thickness of 2 mm. The other modified ceramic membranes, such as those shown in Figure 5, are all based on a 3–5 μm thick layer of γ-alumina modified with different functionalization agents on a 2 mm porous α-alumina layer. In other words, our layers are about 10 times thinner.

In summary, we have reported a facile and efficient membrane modification approach to develop a continuous and defect-free melamine-based microporous organic framework selective layer for OSN applications. Because of the formation of such thin layers (only 360 nm thick), the obtained membranes showed a much higher organic solvent permeability than other state-of-the-art ceramic membranes. A maximum toluene permeability of 7.8 L m^{-2} h^{-1} bar^{-1} was obtained with a MT membrane, the permeability of which is roughly 2.5 times higher than that of the best reported ceramic membranes. In addition, owing to their microporosity, the POF membranes showed excellent rejection values for the organic dyes with a

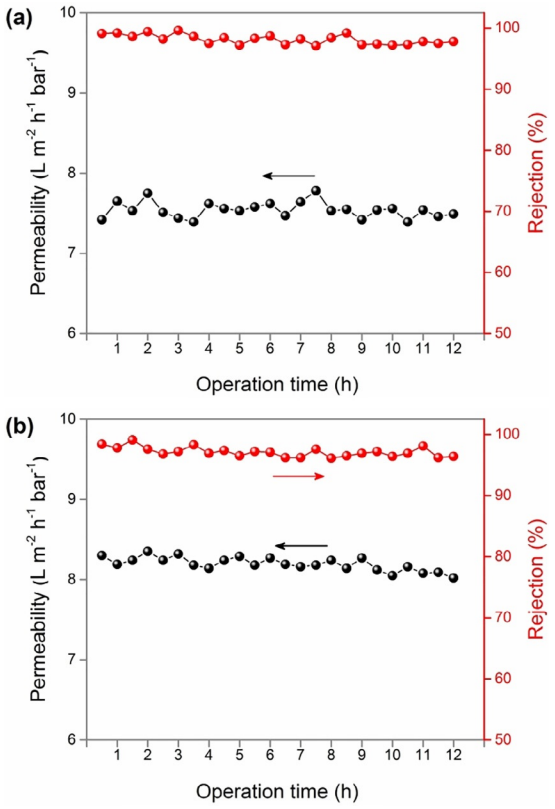

Figure 4. Long-term OSN test of 20 mg L^{-1} (a) Bromothymol Blue/toluene and (b) Bromothymol Blue/*n*-heptane using a MT POF-modified α-alumina membrane.

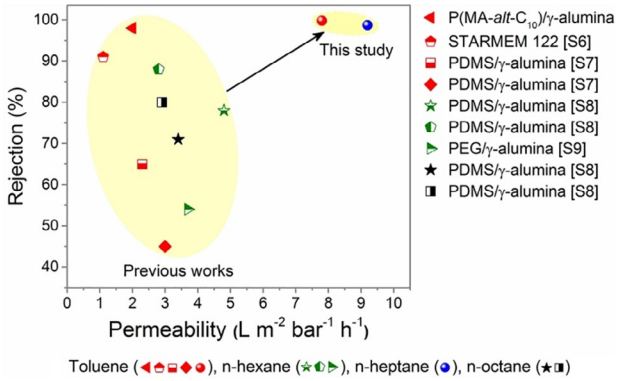

Figure 5. Comparison of the OSN performance for the separation of Sudan Black B of MT POF-modified α-alumina membrane with state-of-the-art ceramic and commercially polymeric ATARMEM 122 membranes (for details, see Table S2).

$M_W > 418$ Da. Furthermore, the POF membranes showed excellent solvent stability with no change in solvent permeation and solute rejection after 12 h of continuous solvent filtration.

Given their superior performance coupled with high solvent stability, the use of POF membranes on an alumina substrate is an attractive choice for purification of nonpolar organic solvents where most of the investigated polymeric membranes failed. Furthermore, as the library of building blocks for (functionalized) organic frameworks is vast and continuously increasing, the tunability of such systems is expected to further increase, paving the way for a wider integration of these frameworks in the field of high-performance OSN applications, addressing various molecular separations.

Acknowledgements

This work is part of the research program entitled "Modular Functionalized Ceramic Nanofiltration Membranes" (BL-20-10), which is taking place within the framework of the Institute for Sustainable Process Technology (ISPT) and is jointly financed by the Netherlands Organization for Scientific Research (NWO) and ISPT, The Netherlands. LCPMdS acknowledges the European Research Council (ERC) for a consolidator Grant, which is part of the European Union's Horizon 2020 research and innovation program (grant agreement No. 682444). BMW acknowledges the NWO Gravitation Program (i.e., MCEC) for financial support.

Conflict of interest

The authors declare no conflict of interest.

Keywords: membranes · microporous materials · organic solvent nanofiltration · polymers · porous organic frameworks

[1] a) G. Szekely, M. F. Jimenez-Solomon, P. Marchetti, J. F. Kim, A. G. Livingston, *Green Chem.* **2014**, *16*, 4440–4473; b) P. Marchetti, M. F. J. Solomon, G. Szekely, A. G. Livingston, *Chem. Rev.* **2014**, *114*, 10735–10806; c) Q. Yang, Y. Su, C. Chi, C. T. Cherian, K. Huang, V. G. Kravets, F. C. Wang, J. C. Zhang, A. Pratt, A. N. Grigorenko, F. Guinea, A. K. Geim, R. R. Nair, *Nat. Mater.* **2017**, *16*, 1198; d) B. Liang, H. Wang, X. Shi, B. Shen, X. He, Z. A. Ghazi, N. A. Khan, H. Sin, A. M. Khattak, L. Li, Z. Tang, *Nat. Chem.* **2018**, *10*, 961–967.

[2] M. Amirilargani, R. B. Merlet, A. Nijmeijer, L. Winnubst, L. C. P. M. de Smet, E. J. R. Sudhölter, *J. Membr. Sci.* **2018**, *564*, 259–266.

[3] L. Huang, J. Chen, T. Gao, M. Zhang, Y. Li, L. Dai, L. Qu, G. Shi, *Adv. Mater.* **2016**, *28*, 8669–8674.

[4] N. Joseph, J. Thomas, P. Ahmadiannamini, H. Van Gorp, R. Bernstein, S. De Feyter, M. Smet, W. Dehaen, R. Hoogenboom, I. F. J. Vankelecom, *Adv. Funct. Mater.* **2017**, *27*, 1605068.

[5] a) S. Karan, Z. Jiang, A. G. Livingston, *Science* **2015**, *348*, 1347–1351; b) Z. Jiang, S. Karan, A. G. Livingston, *Adv. Mater.* **2018**, *30*, 1705973.

[6] a) H. Fan, J. Gu, H. Meng, A. Knebel, J. Caro, *Angew. Chem. Int. Ed.* **2018**, *57*, 4083–4087; *Angew. Chem.* **2018**, *130*, 4147–4151; b) J. Hou, P. D. Sutrisna, Y. Zhang, V. Chen, *Angew. Chem. Int. Ed.* **2016**, *55*, 3947–3951; *Angew. Chem.* **2016**, *128*, 4015–4019.

[7] a) K. Huang, B. Wang, S. Guo, K. Li, *Angew. Chem. Int. Ed.* **2018**, *57*, 13892–13896; *Angew. Chem.* **2018**, *130*, 14088–14092; b) H. Wang, S. He, X. Qin, C. Li, T. Li, *J. Am. Chem. Soc.* **2018**, *140*, 17203–17210; c) J. Y. Chan, H. Zhang, Y. Nolvachai, Y. Hu, H. Zhu, M. Forsyth, Q. Gu, D. E. Hoke, X. Zhang, P. J. Marriot, H. Wang, *Angew. Chem. Int. Ed.* **2018**, *57*, 17130–17134; *Angew. Chem.* **2018**, *130*, 17376–17380.

[8] a) M. Y. Jeon, D. Kim, P. Kumar, P. S. Lee, N. Rangnekar, P. Bai, M. Shete, B. Elyassi, H. S. Lee, K. Narasimharao, S. N. Basahel, S. Al-Thabaiti, W. Xu, H. J. Cho, E. O. Fetisov, R. Thyagarajan, R. F. DeJaco, W. Fan, K. A. Mkhoyan, J. I. Siepmann, M. Tsapatsis, *Nature* **2017**, *543*, 690; b) P.-S. Huang, C. H. Lam, C.-Y. Su, Y.-R. Chen, W.-Y. Lee, D.-M. Wang, C.-C. Hua, D.-Y. Kang, *Angew. Chem. Int. Ed.* **2018**, *57*, 13271–13276; *Angew. Chem.* **2018**, *130*, 13455–13460.

[9] a) P. R. Kidambi, G. D. Nguyen, S. Zhang, Q. Chen, J. Kong, J. Warner, A.-P. Li, R. Karnik, *Adv. Mater.* **2018**, *30*, 1804977; b) G. Wei, X. Quan, S. Chen, H. Yu, *ACS Nano* **2017**, *11*, 1920–1926.

[10] a) X. Zou, G. Zhu, *Adv. Mater.* **2018**, *30*, 1700750; b) Y. Cheng, Y. Ying, S. Japip, S.-D. Jiang, T.-S. Chung, S. Zhang, D. Zhao, *Adv. Mater.* **2018**, *30*, 1802401.

[11] a) D. B. Shinde, G. Sheng, X. Li, M. Ostwal, A.-H. Emwas, K.-W. Huang, Z. Lai, *J. Am. Chem. Soc.* **2018**, *140*, 14342 – 14349; b) V. A. Kuehl, J. Yin, P. H. H. Duong, B. Mastorovich, B. Newell, K. D. Li-Oakey, B. A. Parkinson, J. O. Hoberg, *J. Am. Chem. Soc.* **2018**, *140*, 18200 – 18207.

[12] a) Y. Wang, J. Li, Q. Yang, C. Zhong, *ACS Appl. Mater. Interfaces* **2016**, *8*, 8694 – 8701; b) L.-C. Lin, J. Choi, J. C. Grossman, *Chem. Commun.* **2015**, *51*, 14921 – 14924; c) Y. P. Tang, H. Wang, T. S. Chung, *ChemSusChem* **2015**, *8*, 138 – 147.

[13] a) P. Gorgojo, S. Karan, H. C. Wong, M. F. Jimenez-Solomon, J. T. Cabral, A. G. Livingston, *Adv. Funct. Mater.* **2014**, *24*, 4729 – 4737; b) A. Sabetghadam, X. Liu, A. F. Orsi, M. M. Lozinska, T. Johnson, K. M. B. Jansen, P. A. Wright, M. Carta, N. B. McKeown, F. Kapteijn, J. Gascon, *Chem. Eur. J.* **2018**, *24*, 12796 – 12800.

[14] a) C. H. Lau, K. Konstas, A. W. Thornton, A. C. Y. Liu, S. Mudie, D. F. Kennedy, S. C. Howard, A. J. Hill, M. R. Hill, *Angew. Chem. Int. Ed.* **2015**, *54*, 2669 – 2673; *Angew. Chem.* **2015**, *127*, 2707 – 2711; b) C. H. Lau, X. Mulet, K. Konstas, C. M. Doherty, M.-A. Sani, F. Separovic, M. R. Hill, C. D. Wood, *Angew. Chem. Int. Ed.* **2016**, *55*, 1998 – 2001; *Angew. Chem.* **2016**, *128*, 2038 – 2041; c) X. Wu, M. Shaibani, S. J. D. Smith, K. Konstas, M. R. Hill, H. Wang, K. Zhang, Z. Xie, *J. Mater. Chem. A* **2018**, *6*, 11327 – 11336.

[15] X. Gao, X. Zou, H. Ma, S. Meng, G. Zhu, *Adv. Mater.* **2014**, *26*, 3644 – 3648.

[16] S. Yuan, X. Li, J. Zhu, G. Zhang, P. Van Puyvelde, B. Van der Bruggen, *Chem. Soc. Rev.* **2019**, *48*, 2665 – 2681.

[17] a) M. G. Schwab, B. Fassbender, H. W. Spiess, A. Thomas, X. Feng, K. Müllen, *J. Am. Chem. Soc.* **2009**, *131*, 7216 – 7217; b) P. Puthiaraj, Y.-R. Lee, S. Zhang, W.-S. Ahn, *J. Mater. Chem. A* **2016**, *4*, 16288 – 16311.

[18] a) J. Pan, S. Jia, G. Li, Y. Hu, *Anal. Chem.* **2015**, *87*, 3373 – 3381; b) O. S. Taskin, S. Dadashi-Silab, B. Kiskan, J. Weber, Y. Yagci, *Macromol. Chem. Phys.* **2015**, *216*, 1746 – 1753.

[19] a) C. Wang, Z. Li, J. Chen, Z. Li, Y. Yin, L. Cao, Y. Zhong, H. Wu, *J. Membr. Sci.* **2017**, *523*, 273 – 281; b) C. Li, S. Li, L. Tian, J. Zhang, B. Su, M. Z. Hu, *J. Membr. Sci.* **2019**, *572*, 520 – 531.

[20] a) G. Delen, Z. Ristanović, L. D. B. Mandemaker, B. M. Weckhuysen, *Chem. Eur. J.* **2018**, *24*, 187 – 195; b) D. Fu, K. Park, G. Delen, Ö. Attila, F. Meirer, D. Nowak, S. Park, J. E. Schmidt, B. M. Weckhuysen, *Chem. Commun.* **2017**, *53*, 13012 – 13014; c) L. D. B. Mandemaker, M. Filez, G. Delen, H. Tan, X. Zhang, D. Lohse, B. M. Weckhuysen, *J. Phys. Chem. Lett.* **2018**, *9*, 1838 – 1844.

[21] a) L. M. Sharaf, M. M. El Nady, *Pet. Sci. Technol.* **2006**, *24*, 607 – 627; b) H.-G. Franck, J. W. Stadelhofer, *Industrial Aromatic Chemistry*, Springer, Berlin, Heidelberg, **1988**, pp. 236 – 264.

[22] H. H. Funke, A. M. Argo, C. D. Baertsch, J. L. Falconer, R. D. Noble, *J. Chem. Soc. Faraday Trans.* **1996**, *92*, 2499 – 2502.

[23] C. D. Baertsch, H. H. Funke, J. L. Falconer, R. D. Noble, *J. Phys. Chem.* **1996**, *100*, 7676 – 7679.

[24] S. Darvishmanesh, J. Degrève, B. Van Der Bruggen, *Phys. Chem. Chem. Phys.* **2010**, *12*, 13333 – 13342.

Manuscript received: August 26, 2019
Revised manuscript received: September 20, 2019
Accepted manuscript online: September 28, 2019
Version of record online: October 18, 2019

